J Mol Model (2009) 15:1299–1315
DOI 10.1007/s00894-009-0495-0

ORIGINAL PAPER

Theoretical investigations on the hydrolysis pathway of tin verdoheme complexes: elucidation of tin's ring opening inhibition role

Mahdi D. Davari · Homayoon Bahrami · Mansour Zahedi · Nasser Safari

Received: 17 January 2009 / Accepted: 25 February 2009 / Published online: 17 April 2009

Abstract In order to obtain a better molecular understanding of inhibitory role of tin metal in the verdoheme ring opening process, hydrolysis of three possibly six, five, and four coordinate verdoheme complexes of tin(IV) and (II) have been studied using DFT method. The results of calculations indicate that, in excellent accord with experimental reports, hydrolysis of different possibly coordinated tin(IV) and (II) verdohemes does not lead to the opening of the macrocycle. Contrary to iron and zinc verdohemes, in five and four coordinate verdoheme complexes of tin(IV) and (II), formation of open ring helical complexes of tin are unfavorable both thermodynamically and kinetically. In these pathways, coordination of hydroxide nucleophile to tin metal due to the highly charged, exclusive oxophilicity nature of the Sn center, and high affinity of Sn to increase coordination state are proposed responsible as inhibiting roles of tin *via* the ring opening. While, in saturated six coordinate tin(IV) and (II) verdoheme complexes the ring opening of tin verdohemes is possible thermodynamically, but it is not predicted to occur from a kinetics point of view. In the six coordinate pathway, tin plays no coordination role and direct addition of hydroxide nucleophile to the positive oxo-carbon centers and formation of closed ring hydroxy compounds is proposed for preventing the verdoheme ring opening. These key points and findings have been corroborated by the results obtained from atomic charge analysis, geometrical parameters, and molecular orbital calculations. In addition, the results of inhibiting ring opening reaction of tin verdoheme complexes could support the great interest of tin porphyrin analogues as pharmacologic means of chemoprevention of neonatal jaundice by the competitive inhibitory action of tin porphyrins on heme oxygenase.

Keywords Competitive inhibitor · DFT · Heme degradation · Hydrolysis · Ring opening · Neonatal jaundice · Tin porphyrin · Tin verdoheme

Electronic supplementary material The online version of this article (doi:10.1007/s00894-009-0495-0) contains supplementary material, which is available to authorized users.

M. D. Davari · H. Bahrami · M. Zahedi (✉) · N. Safari
Department of Chemistry, Faculty of Sciences,
Shahid Beheshti University,
G.C., Evin,
19839-6313 Tehran, Iran
e-mail: m-zahedi@cc.sbu.ac.ir

Introduction

Heme oxygenase (HO) catalyzes the catabolism of heme to biliverdin, CO and free iron through three successive oxygenation steps, in which the heme group functions as the prosthetic group as well as the substrate (Scheme 1) [1–5]. The third oxygenation, the verdoheme ring opening, has been the least understood step in the HO catalysis, even though this step is considered as the rate-determining step to regulate HO enzyme activity *in vivo* [6]. The biological action of heme oxygenase can be mimicked chemically by the process of coupled oxidation [7–11]. It is reported that metal complex of 5-oxa-porphyrin macrocycle "verdoheme" is also generated as a detectable intermediate during inductive cleavage process of heme by HO [1–6, 10, 11]. The mechanism that converts verdoheme into biliverdin has been the subject of controversy [1–5, 11–13]. One possible path for conversion of verdoheme into biliverdin includes hydrolysis of 5-oxa-porphyrin macrocycle [1, 2, 8–11, 14–16]. Recent experimental results have shown that addition of nucleophile to Fe(II), Co(II), and Zn(II) verdohemes result in the ring opening in the macrocycle and leads to the

Scheme 1 Heme oxygenase reaction; V=Vinyl, Me=Methyl, Pr=Propionate

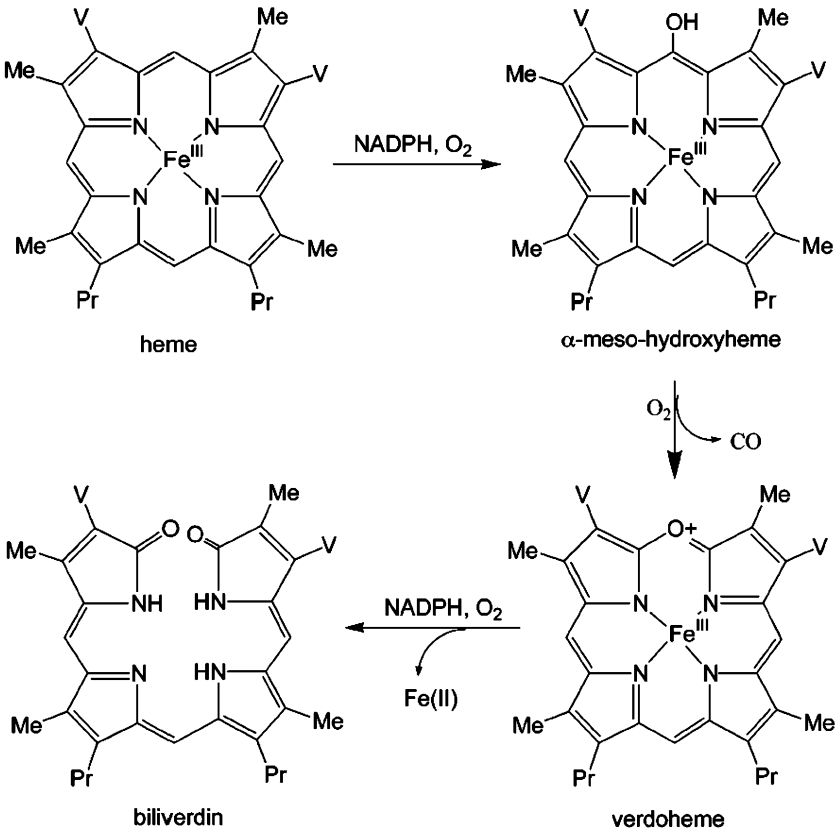

opened metal biliverdin complexes [16–19]. These results may support the possibility of hydrolysis path in biological process, as well. It has been proposed that these reactions are done by nucleophilic attack at one of the carbon atoms adjacent to the oxygen of verdoheme ring, where a tetrahedral carbon atom is initially formed followed by the ring opening process [18, 19]. While, ring opening process of metalloporphyrins has been observed to take place with metals such as Mn, Fe, Co, and Zn, some other metals like Sn prevent ring opening [20].

A particularly useful property of tin complexes of meso- and proto-porphyrins and their analogues is their competitive inhibition of heme oxygenase, making them candidates for the treatment of hyperbilirubinemia [21–30]. It has also been proposed that these compounds bind to heme oxygenase far more avidly than does heme itself, thus blocking access of the natural substrate to the binding site of the enzyme and inhibiting heme degradation and bilirubin production [26]. However, there are some ambiguities regarding interaction of Sn porphyrin analogues with heme protein in aforementioned process [31–33]. In spite of the considerable experimental research performed on heme degradation and its inhibition in the past few years [23–30, 34, 35], theoretical modeling of verdoheme degradation process has received little attention [36–39]. Especially, the roles of tin metal including coordination, oxidation states and also effects of axial ligand is not elucidated during the preventing ring opening process. Whereas, the understanding of ring opening inhibition at the molecular level is of particular importance in drug development and drug therapy [40, 41].

Our early work on the conversion of zinc verdoheme into biliverdin in accord with experimental report [17], showed that presence of the zinc atom leads to the increase of positive charge on carbon atoms adjacent to the oxygen atom in zinc verdoheme relative to 5-oxa-porphyrin [42]. It was determined that an intermediate is initially formed by nucleophilic attack on one of the aforementioned carbon atoms. This intermediate was then directly converted to a helical open-ring complex of zinc biliverdin. Even though the most positive center for the nucleophile to attack was the zinc ion of zinc(II) verdoheme, it was shown that such addition did not lead to a stable intermediate. Thus, the zinc atom had no coordination role in transferring the nucleophiles to the oxo carbon, but it just had the effect of activating the oxo carbon for nucleophile addition. Also a more recent work in fair agreement with experimental reports has shown that direct nucleophilic addition to the five coordinate iron(II) verdoheme macrocycle is a possible mechanism for conversion of verdoheme to biliverdin [43]. According to these results, the role of metal and ligand coordination in heme degradation is important.

Studies with synthetic metalloporphyrin complexes in which the central iron atom of heme is replaced by tin indicate that these heme analogues that cannot be enzymatically degraded to bile pigment possess novel biological properties that may have considerable clinical as well as experimental values [25]. However, the oxidation state of Sn is not resolved clearly *in vivo*, and there is possibility for Sn(IV) reduction to Sn(II) in the reductive environment of body. Because the role of Sn in the course of reaction is not yet known [44], its different coordination with various oxidation states is considered in this study. So, this work is an attempt to further explore the biological actions and metabolic disposition of Sn verdohemes, in order to investigate the possible pathways for its inhibitory role in verdoheme ring opening process. To do so, we have examined hydrolysis pathway of a model system of tin (IV) and (II) verdohemes complexes with three different possible coordination states of tin, namely Sn with six, five, and four coordination to tin(IV) and (II) biliverdin complexes using B3LYP density functional method. Results of the theoretical method have been used to predict the structural and energetic properties of tin verdoheme complexes with various oxidation states and coordinations, where we also present analyses of various pathways. A discussion of the obtained results is followed by possible implications of the inhibitory effects and role of tin metal in these reactions from different views.

Computational details

In most of previous reports, it is clearly explained that a DFT method is useful to determine catalytic cycles in biological organisms [45–47]. Based on conclusions drawn from our previous works [42, 43, 48, 49], and since several studies [50, 51] have demonstrated that reliable quantitative results are obtained at this level of theory, we have used B3LYP [52–54] method. No side-chains were attached to the verdoheme models evaluated in this study in order to keep the calculation size manageable. Imidazole, hydroxyl and porphyrin have been considered as models of ligand in meso- and proto-porphyrin IX. All structures were optimized using B3LYP method while employing 3-21G [55] basis set for Sn and 6-31G [56] basis set for remaining atoms, namely O, N, C and H. Also, energies of all optimized geometries were calculated using the 3-21G basis set for Sn and 6-31G(d) [57] basis set for other atoms at the B3LYP level. Full geometry optimizations and energy calculations were performed by means of the GAUSSIAN 98 program [58] without any symmetry constraint imposed. Zero point-energy corrections were taken into account for calculating the energetics of the reaction pathways. Basis set superposition errors (BSSE) were evaluated using the counterpoise method [59]. Systematic vibrational frequency analyses on all species studied confirm the minima geometries and transition states on their corresponding potential surfaces by having zero and one imaginary frequency respectively. Furthermore, in one case, hydrolysis pathway of four coordinate Sn(IV) verdoheme, we extended our calculations to B3LYP/LANL2DZ [60] for the geometry optimization and energy calculations and no differences in the geometrical parameters and energy level orders were observed.

Results

Hydrolysis of the six coordinate Sn(IV) and (II) verdohemes

Proposed mechanism of hydrolysis pathway for six coordinate Sn(IV) and (II) verdohemes with imidazole and hydroxyl as fifth and sixth axial ligands, $[Sn^{IV}(OP)(IM)(OH)]^{2+}$ and $[Sn^{II}(OP)(IM)(OH)]$, (OP and IM are mono anion of 5-oxa-porphyrin and neutral imidazole ligands respectively) has been shown in Scheme 2. The numbering system of this scheme has been used for charge analysis of verdoheme and comparison of structural variations in the course of reaction. It is established that the heme in heme-HO complex is coordinated by a proximal histidine residue and by distal OH^- or water [10, 61, 62]. So, one of the axial ligands in the model system could be neutral imidazole and it would be very interesting to investigate the orientation of axially coordinated imidazole. To assess the influence of orientation of neutral axially ligated imidazole we scanned the N1–Sn–N5–C5 dihedral angle in $[Sn^{IV}(OP)(IM)(OH)]^{2+}$ model system. Such analysis shows that those conformations of six coordinate Sn(IV) verdoheme are the most stable ones, in which their imidazole ring is parallel to N1–Sn–N3 or N2–Sn–N4 diametrical lines while the non-ligated N6 of imidazole is far from the verdoheme O1 oxygen. In the least stable conformer the N5–C5 is located above the Sn–N3 or Sn–N4 while there is a close interaction between N6 and O1. Required energy for free rotation over bond between Sn and N5 of imidazole was calculated and it turned out to have a small amount of 0.8 $kcal.mol^{-1}$. Thus, the rotation barrier is less than 1 $kcal.mol^{-1}$ and is not high enough to justify preference of a conformer versus another. However, such orientation of planar imidazole ring in verdoheme could play a critical role in nucleophilic reaction, when OH^- attacks oxo-carbons in six and five coordinate verdohemes with a *cis* position relative to imidazole ligand.

Calculated Mulliken atomic charges for optimized structures of tin(IV) and (II) verdohemes, are summarized in Table 1. For comparison, the Mulliken atomic charges of optimized 5-oxa-porphyrin (OP) have been offered in the same table. Data of this table reveal that the most positive

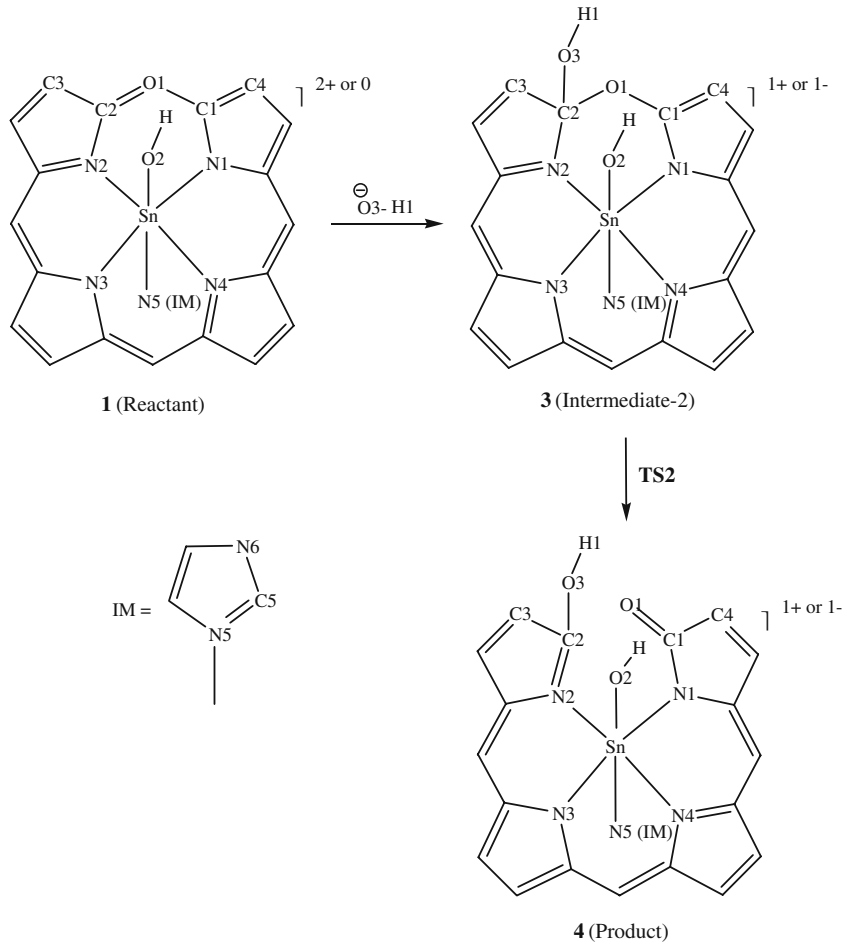

Scheme 2 A perspective view and numbering system of the product of OH^- addition to six coordinate $[Sn^{IV}(OP)(IM)(OH)]^{2+}$ or $[Sn^{II}(OP)(IM)(OH)]$ (**1**) as either macrocycle (**3**) or as open-chain tetrapyrrol (**4**); Imidazole (IM) and OH^- are fifth and sixth axial ligands respectively

centers of $[Sn^{IV}(OP)(IM)(OH)]^{2+}$ are located at Sn and two carbon atoms adjacent to oxygen with positive charges equal to 2.14 and 0.54 respectively. The corresponding positive charges on Sn and oxo carbons in $[Sn^{II}(OP)(IM)(OH)]$ are 2.00 and 0.51 respectively. The calculated positive charge for these carbons on 5-oxa-porphyrin macrocycle is 0.50. Thus, based on results of Table 1 and similar to our previous studies [42,43], Sn and C1 or C2 atoms are the best electrophilic positions for nucleophilic addition. Although the reaction of ion pairs occurs when

Table 1 Mulliken atomic charges for 5-oxa-porphyrin (OP) and optimized geometries of six, five, and four coordinate Sn(IV) and (II) verdohemes

		Sn(IV) verdoheme			Sn(II) verdoheme		
Atom	OP	six coordinate	five coordinate	four coordinate	six coordinate	five coordinate	four coordinate
Sn	-	2.14	2.01	1.91	2.00	1.95	1.73
O1	-0.57	-0.43	-0.41	-0.40	-0.53	-0.52	-0.50
C1	0.50	0.54	0.55	0.57	0.51	0.51	0.54
C2	0.50	0.54	0.56	0.57	0.52	0.51	0.54
N1	-0.46	-0.78	-0.79	-0.80	-0.77	-0.80	-0.79
N2	-0.46	-0.78	-0.78	-0.80	-0.77	-0.79	-0.79
N3	-0.48	-0.83	-0.83	-0.84	-0.83	-0.85	-0.84
N4	-0.48	-0.83	-0.82	-0.84	-0.82	-0.84	-0.84
Imidazole	-	0.28	0.48	-	0.14	0.28	-
N5(IM)	-	-0.63	-0.65	-	-0.50	-0.60	-
O2	-	-0.84	-	-	-0.83	-	-

they are charged, it has not been common practice to explicitly describe the counter ions in the electronic structure calculations. Because the complexes are six coordinate and Sn is saturated, OH^- can only directly attack one of the 5-oxo carbons in this pathway. So these reactions pathway are initiated by the direct attack of the OH^- nucleophile on the oxo carbons as shown in Scheme 2. In accord with proceeding experimental reports, a compound that might arise from nucleophilic addition to each carbon adjacent to oxygen atom of **1**s is called intermediate-2 (Int2 or compound **3**). Also, based on available experimental data for Zn and Fe [16–18] and our previous results [42, 43] final products of the reactions should be six coordinate open-ring helical hydroxy tetrapyrrol species (**4**), which are generated from the C2–O1 bond cleavages in intermediate-2s as shown in Scheme 2. Geometries of all species during the ring opening process including reactants (**1**s), intermediate-2s (**3**s) and products (**4**s) have been determined and optimized. Also, transition states (**TS2**s) between intermediates and products have been located and optimized.

OH^- can attack the six coordinate tin verdoheme model ending up with two positions of *cis* and *trans* moieties relative to imidazole ring. Results obtained show that the *trans* addition of OH^- to $[Sn^{IV}(OP)(IM)(OH)]^{2+}$ produces a compound which is about 5.9 kcal.mol^{-1} more stable than an intermediate that might arise from that of *cis*. So, *trans* attack on oxo carbons while the steric effect of imidazole is minimized can be energetically preferred. Note that in order to correct reactants energies, basis set superposition errors were calculated and turned out to have amounts of 14.0 and 11.1 kcal.mol^{-1}, respectively. Subsequently, energies of all above optimized geometries have been calculated and summarized in Table 2. In this table, energy of compounds **3** has been chosen as zero energy for six coordinate paths.

By taking a look at this table, it is clear that **3**s are generated in exothermic processes by the energy release of 247.8 and 78.7 kcal.mol^{-1}, and products (**4**s) are 10.1 and 21.2 kcal.mol^{-1} more stable than the closed ring hydroxy intermediates (**3**s) in Sn(IV) and Sn(II) paths, respectively. Also barrier energies for passing over transition structures (**TS2**s) between **3**s and **4**s show significant amounts of 38.6 and 45.0 kcal.mol^{-1}, respectively.

In order to investigate main geometrical variations during hydrolysis of tin(IV) and (II) verdohemes, some geometrical parameters were chosen and their values for all species have been summarized in Table 3. As shown in Table 3, Sn–Ni (i=1-4) bond distances and Ni–Sn–Nj (i,j=1-4) bond angles as well as N1–N2–N3–N4 dihedral angle have been employed for showing the tin atom's position in the verdoheme ring. Also, the sum of four bond angles over two Sn–N bonds can be a criterion for planarity of porphyrin ring [63]. Besides, planarity of the porphyrin ring could be indicated by C1–O1, C2–O1, C1–O1–C2, N2–C2–O1, and C3–C2–O1 angles as well as N1–Sn–N2–C2 and N2–Sn–N1–C1 dihedral angles. Moreover, some parameters such as Sn–N5, Sn–O2 bond distances and N1–Sn–N5, N2–Sn–N5, N1–Sn–O2, and N2–Sn–O2 bond angles have been included which show the positions of imidazole (IM) and OH^- ligands relative to verdoheme ring and each other. C2–O3, O1–O3, C3–C2–O3, O3–C2–O1, C2–O3–H1, and N2–C2–O3–H1 show position of OH^- nucleophile relative to verdoheme ring in **3**s, **TS2**s, and **4**s, respectively. Regarding value of C3–C2–O3–H1, it may be used to inquire whether OH^- nucleophile is coplanar with its adjacent pyrrole ring. These structural parameters have been chosen and will be compared to those of hydrolysis reactions of five (Table 4) and four (Table 5) coordinate tin (IV) and (II) verdohemes in the next sections.

Hydrolysis of the five coordinate Sn(IV) and (II) verdohemes

A mechanism belonging to adding hydroxide ion to five coordinate Sn(IV) and (II) verdohemes with an imidazole ligand has been displayed in Scheme 3, because there is a tendency to present a five coordinate structure of central metal in heme oxygenase [10, 61, 62]. In this scheme, a numbering system of some atoms for **1**s is maintained for these atoms in intermediates, transition states and products that arise from nucleophilic attack to **1**s.

Table 2 Calculated relative energies for species in the hydrolysis of variously coordinated tin (IV) and (II) verdohemes and conversion to tin biliverdins; IM and OH^- are fifth and six axial ligands, respectively

	Energy stabilization (kcal.mol^{-1})					
Compounds	**1**+ OH^- *	**2**	**TS1**	**3**	**TS2**	**4**
$[Sn^{IV}(OP)(IM)(OH)]^{2+}$	247.8	-	-	0.0	38.6	-10.1
$[Sn^{II}(OP)(IM)(OH)]$	78.7	-	-	0.0	45.0	-21.2
$[Sn^{IV}(OP)(IM)]^{3+}$	333.6	0.0	32.0	10.4	18.0	-3.8
$[Sn^{II}(OP)(IM)]^{+}$	162.8	0.0	39.7	12.7	28.7	-9.2
$[Sn^{IV}(OP)]^{3+}$	393.9	0.0	51.9	42.6	51.0	29.3
$[Sn^{II}(OP)]^{+}$	222.4	0.0	73.2	22.2	69.9	34.1

* Basis set superposition errors have been included.

Table 3 Selected bond lengths, bond angles, and dihedral angles for reactants, intermediates, transition states and products which might arise from addition of OH^- to six coordinate tin(IV) and (II) verdohemes

	Sn(IV)				Sn(II)			
	1	**3**	**TS2**	**4**	**1**	**3**	**TS2**	**4**
Bond distance(Å)								
Sn–N1	2.11	2.10	2.10	2.16	2.11	2.12	2.13	2.21
Sn–N2	2.10	2.06	2.07	2.19	2.11	2.06	2.09	2.21
Sn–N3	2.09	2.08	2.09	2.18	2.10	2.11	2.10	2.17
Sn–N4	2.09	2.08	2.07	2.16	2.10	2.08	2.10	2.17
Sn–N5	2.28	2.31	2.21	2.26	2.37	2.34	2.40	2.29
Sn–O2	1.99	2.05	2.22	2.00	2.01	2.07	2.03	2.02
C1–O1	1.36	1.35	1.31	1.25	1.39	1.29	1.29	1.31
C2–O1	1.36	1.53	1.90	2.94	1.39	1.56	1.57	3.00
C2–O3	-	1.38	1.39	1.35	-	1.41	1.44	1.37
Bond angle(°)								
N1–Sn–N2	86.7	88.1	91.8	101.5	86.6	89.1	87.3	102.0
N2–Sn–N3	90.2	90.0	87.7	85.9	164.5	89.3	90.5	86.6
N1–Sn–N3	169.4	167.3	176.1	160.1	164.5	162.9	160.4	157.5
N2–Sn–N4	170.2	176.8	168.2	171.6	166.0	174.7	168.1	171.3
N4–Sn–N1	89.9	91.3	91.3	86.9	90.2	89.9	88.7	86.7
N1–Sn–N5	84.8	83.5	88.0	82.8	83.0	81.3	80.4	80.7
N2–Sn–N5	85.3	89.0	93.8	86.6	82.0	86.2	84.2	84.9
C1–O1–C2	128.8	120.8	120.1	110.1	126.2	115.4	115.2	113.1
N1–Sn–O2	93.3	89.7	87.3	98.2	96.3	91.3	100.6	95.8
N2–Sn–O2	87.4	83.9	81.1	92.9	92.9	85.2	97.5	89.7
N2–C2–O1	124.8	109.8	109.3	88.7	125.6	108.9	109.2	88.5
C3–C2–O1	123.4	109.5	106.1	118.1	123.0	108.7	110.7	126.5
C3–C2–O3	-	113.0	123.3	129.0	-	114.5	110.1	126.6
O3–C2–O1	-	108.5	94.1	67.5	-	106.7	105.1	88.7
C2–O3–H1	-	111.3	114.0	114.1	-	109.0	109.1	106.1
Dihedral angle(°)								
N1–N2–N3–N4	-0.6	-6.7	-10.8	-13.6	-1.1	-8.6	-5.7	-14.9
N2–Sn–N1–C1	11.3	-1.1	14.6	12.9	-11.2	-2.4	2.3	11.2
N1–Sn–N2–C2	-12.1	32.1	20.7	35.8	10.7	28.1	20.8	39.1
N2–C2–O3–H1	-	-21.5	-177.1	-163.1	-	-13.6	-66.1	-72.1
C3–C2–O3–H1	-	-137.8	48.5	20.9	-	-132.9	-174.4	107.3

By taking a look at results of Mulliken atomic charge analysis as summarized in Table 1, it is clear that the least charge density of $[Sn^{IV}(OP)(IM)]^{3+}$ and $[Sn^{II}(OP)(IM)]^{+}$ are centered on each of the carbons adjacent to O2 of verdoheme ring and Sn with positive average values equal to 0.55, 0.51 and 2.01, 1.95, respectively. Thus, in accord to previous section and experimental reports, latter atoms can be considered as centers for OH^- addition. Compounds that are produced from OH^- nucleophilic attack to Sn and each oxo-carbons of **1**s are called intermediate-1 (**2**) and intermediate-2 (**3**), and **4**, respectively. Note that Sn is six coordinate in intermediate-1s in this pathway and OH^- can be shifted to oxo carbons (intermediate-2s) by a rebound mechanism. Geometry of intermediates as well as helical opened ring compounds as final products arise from hydrolysis of **1**s have been determined and optimized. Also, transition states between intermediates and for passing from intermediate-2s to products have been located and their geometries optimized. In accord with previous results [42, 43], latter transition states have been called **TS1** and **TS2**, respectively.

It is noteworthy that in a similar way to six coordinate verdoheme in production of intermediate-2s, OH^- can be added to oxo-carbons in two positions relative to imidazole ring, namely *cis* and *trans* positions. Results obtained indicate that an intermediate that is produced from OH^- attack with a *trans* position relative to imidazole ring in $[Sn^{IV}(OP)(IM)]^{3+}$ is about 6 $kcal.mol^{-1}$ more stable than that of *cis* position. So, similar to six coordinate pathways, *trans* addition to oxo carbons while the steric effect of

Table 4 Selected bond lengths, bond angles, and dihedral angles for reactants, intermediates, transition states and products which might arise from OH^- nucleophilic addition to five coordinate tin(IV) and (II) verdohemes

	Sn(IV)						Sn(II)					
	1	**2**	**TS1**	**3**	**TS2**	**4**	**1**	**2**	**TS1**	**3**	**TS2**	**4**
Bond distance(Å)												
Sn–N1	2.11	2.11	2.10	2.10	2.09	2.08	2.09	2.10	2.08	2.05	2.09	2.09
Sn–N2	2.11	2.11	2.10	2.05	2.06	2.12	2.09	2.09	2.05	2.09	2.06	2.09
Sn–N3	2.09	2.09	2.08	2.08	2.09	2.12	2.08	2.08	2.09	2.08	2.09	2.10
Sn–N4	2.09	2.09	2.08	2.07	2.07	2.11	2.08	2.08	2.05	2.07	2.07	2.09
Sn–N5	2.13	2.28	2.18	2.16	2.15	2.15	2.16	2.39	2.20	2.15	2.15	2.19
Sn–O2	-	1.98	2.29	3.51	3.52	3.44	-	1.95	3.56	3.51	3.52	3.49
C1–O1	1.35	1.36	1.37	1.36	1.3	1.25	1.39	1.43	1.39	1.36	1.30	1.28
C2–O1	1.35	1.36	1.4	1.48	1.89	3.2	1.39	1.43	1.53	1.48	1.89	3.16
C2–O2	-	-	1.80	1.42	1.36	1.34	-	-	1.80	1.44	1.36	1.37
Bond angle(°)												
N1–Sn–N2	84.3	86.6	90.8	87.0	90.0	97.7	86.4	46.3	90.8	89.6	90.0	97.3
N3–Sn–N4	88.9	91.2	90.7	89.9	89.7	86.7	88.9	88.9	90.7	90.3	89.7	87.4
N1–Sn–N3	154.9	169.7	173.5	166.0	171.6	173.3	161.4	165.2	176.1	166.0	171.6	175.2
N2–Sn–N4	152.5	170.0	174.8	151.3	147.7	137.1	157.9	163.3	154.4	151.3	147.7	140.2
N1–Sn–N5	102.5	85.0	91.6	96.6	94.6	96.6	97.1	81.9	93.7	96.6	94.6	93.3
N2–Sn–N5	102.9	85.1	91.9	104.8	106.0	107.2	99.2	81.4	101.5	104.8	106.0	106.2
C1–O1–C2	127.9	128.5	123.0	117.9	116.2	-	120.7	113.2	123.0	113.9	116.2	88.3
N2–C2–O1	124.4	124.8	121.7	34.2	107.4	80.4	122.3	122.3	121.7	111.5	107.4	76.7
C3–C2–O1	126.3	-	116.8	110.6	104.4	118.4	125.6	126.1	116.8	109.6	104.4	116.8
C3–C2–O2	-	123.5	113.5	115.1	123.7	129.1	-	-	113.5	115.3	123.7	127.4
O2–Sn–N1	-	90.7	75.3	-	-	-	-	100.0	75.3	-	-	-
O2–C2–O1	-	-	103.8	117.9	96.1	72.6	-	-	103.8	106.2	96.2	78.3
C2–O2–H1	-	-	122.1	112.9	114.2	114.4	-	-	122.1	109.8	114.2	114.1
Dihedral angle(°)												
N1–N2–N3–N4	1.7	0.2	-1.0	10.1	16.7	28.0	2.5	1.4	-15.1	10.1	-16.7	29.1
N2–Sn–N1–C1	13.6	-12.6	-12.3	19.2	26.1	48.1	14.2	-8.0	17.8	19.2	21.2	44.6
N1–Sn–N2–C2	-15.0	11.5	41.3	10.2	11.5	16.1	-15.9	10.6	4.4	10.2	11.5	16.9
N2–C2–O2–H1	-	-	-	162.5	173.7	179.2	-	-	-	-171.7	173.7	-84.6
C3–C2–O2–H1	-	-	-	47.6	37.9	0.1	-	-	-	70.5	38.0	103.5

imidazole is minimum is energetically preferred. Such fact has been mentioned in previous studies [43, 49]. Ultimately, relative energies of all optimized geometries have been calculated and summarized in Table 2. Included basis set superposition errors have amounts of 14.7 and 13.9 kcal.mol^{-1}, respectively. The energy of **2**s has been chosen as zero energies. By taking a look at Table 2, it is obvious that **2**s are produced in exothermic processes by the energy release of 333.6 and 162.8 kcal.mol^{-1}, respectively. These intermediates are more stable than **3**s by 10.4 and 12.7 kcal.mol^{-1} while products are 3.8 and 9.2 kcal.mol^{-1} more stable than **2**s respectively. By taking a closer look at Table 2, it is revealed that barrier energies for conversion of **2**s to **3**s (**TS1**s) have significant values of 32.0 and 39.7 kcal.mol^{-1}, respectively. On the other hand, the expected products are generated from **3**s by passing over transition states (**TS2**s) with calculated barriers of 7.6 and 16.0 kcal.mol^{-1}, respectively.

For the purpose of investigating major geometrical changes during the course of nucleophilic addition of OH^- to **1**s, some selected geometrical parameters with their values for all species including reactants, intermediates, transition states and products have been summarized in Table 4. These structural parameters have been chosen similar to six coordinate tin verdohemes and will be compared to those of hydrolysis reaction of six and four coordinate tin(IV) and (II) verdohemes in the next sections (Tables 3 and 5). Among these parameters, Sn–O2, and O2–Sn–N1 parameters have been included to show the position of OH^- nucleophile relative to Sn center in **2**s.

Table 5 Selected bond lengths, bond angles, and dihedral angles for reactants, intermediates, transition states and products which might arise from OH^- attack to four coordinate tin(IV) and (II) verdohemes

	Sn(IV)						Sn(II)					
	1	**2**	**TS1**	**3**	**TS2**	**4**	**1**	**2**	**TS1**	**3**	**TS2**	**4**
Bond distance(Å)												
Sn–N1	2.06	2.12	2.09	2.08	2.05	2.03	2.07	2.12	2.09	2.33	2.05	2.03
Sn–N2	2.06	2.12	2.06	2.03	2.04	2.07	2.07	2.12	2.06	2.24	2.04	2.05
Sn–N3	2.04	2.11	2.08	2.06	2.04	2.04	2.05	2.11	2.08	2.28	2.05	2.03
Sn–N4	2.04	2.11	2.06	2.05	2.05	2.05	2.05	2.11	2.06	2.31	2.05	2.05
Sn–O2	-	1.94	2.32	3.18	3.33	3.30	-	1.98	2.32	3.31	3.33	3.26
C1–O1	1.35	1.35	1.37	1.36	1.29	1.24	1.38	1.39	2.06	1.36	1.29	1.26
C2–O1	1.35	1.35	1.41	1.47	1.86	3.41	1.38	1.39	2.08	1.48	1.86	1.38
C2–O2	-	-	1.65	1.42	1.36	1.34	-	-	1.65	1.43	1.36	1.38
Bond angle(°)												
N1–Sn–N2	87.4	83.1	87.1	87.0	91.3	106.3	87.1	84.1	87.1	50.2	91.3	104.8
N3–Sn–N4	91.9	87.6	89.5	90.1	90.6	90.8	91.1	86.4	89.5	78.3	90.6	90.8
N1–Sn–N3	177.7	148.8	155.3	154.5	154.4	150.2	178.0	150.5	156.3	120.4	154.4	153.4
N2–Sn–N4	177.8	148.8	158.8	168.3	176.4	149.5	178.0	150.5	158.8	130.7	176.4	147.0
C1–O1–C2	129.5	127.3	121.2	120.5	120.8	97.9	126.0	121.7	121.3	122.3	103.6	92.1
N2–C2–O1	123.8	124.6	118.6	111.8	106.4	72.8	125.2	123.8	30.5	115.0	106.4	76.4
C3–C2–O1	124.3	122.6	115.1	109.9	104.0	111.2	123.4	124.1	115.1	106.2	104.0	111.3
C3–C2–O2	-	-	116.7	117.5	125.6	132.0	-	-	116.7	115.4	125.6	133.0
O2–Sn–N1	-	99.4	78.5	-	-	-	-	101.7	78.5	-	-	-
O2–C2–O1	-	-	104.9	108.5	97.0	83.4	-	-	104.9	106.2	97.0	82.2
C2–O2–H1	-	-	119.1	113.9	115.1	115.8	-	-	119.1	109.8	115.1	112.7
Dihedral angle(°)												
N1–N2–N3–N4	0.0	0.1	-2.6	-9.7	-20.2	-42.1	0.0	0.0	-2.6	-7.7	-20.2	-41.5
N2–Sn–N1–C1	0.0	21.7	22.6	3.9	-7.7	-37.5	0.0	22.4	22.5	24.8	-7.7	158.8
N1–Sn–N2–C2	0.0	-22.0	-52.7	-35.4	-32.5	-37.0	0.0	-22.4	-52.7	-51.7	-32.5	-30.2
N2–C2–O2–H1	-	-	-	-165.1	-174.1	-179.1	-	-	-	175.1	-174.0	158.8
C3–C2–O2–H1	-	-	-	-50.3	-38.2	1.2	-	-	-	-66.5	-38.2	-23.8

Hydrolysis of the four coordinate Sn(IV) and (II) verdohemes

As can be seen in Scheme 3 the proposed mechanism for hydroxide addition to four coordinate Sn(IV) and Sn(II) verdohemes is the same as five coordinate paths. In this scheme, a numbering system of some atoms for $[Sn^{IV}(OP)]^{3+}$ and $[Sn^{II}(OP)]^{+}$ is maintained for these atoms in intermediates, transition states and products that arise from OH^- nucleophilic attack to **1**s. Mulliken atomic charges belonging to optimized geometry of **1**s are summarized in Table 1. By taking a look at this table, it is revealed that similar to previous sections the positions of the least atomic charges in the latter compounds are centered on Sn and two carbon atoms adjacent to oxygen. So, atomic charge of Sn and each oxo-carbon have positive values equal to 1.91, 0.57, and 1.73, 0.54, for Sn(IV) and Sn(II), respectively. Thus, based on results of Table 1 and similar to our previous sections, Sn and C1 or C2 atoms are the best positions for nucleophile addition. Compounds numbering that might arise from nucleophilic attack on Sn and C1 or C2 are the same as five coordinate pathway. Molecular geometries of intermediates, transition states and products in these reactions have been determined and optimized. Thereafter, energies of all species have been calculated and summarized along the reaction coordinate in Table 2. Basis set superposition errors are calculated and turn out to have amounts of 16.6 and 13.5 kcal.mol^{-1} for Sn (IV) and Sn(II), respectively. The reported energies are relative to the zero energy of compounds **2** while basis set superposition errors have been included. By taking a look at Table 2, it is obvious that productions of **2**s are exothermic by about 393.9 and 222.4 kcal.mol^{-1}, respectively. Compound **2**s are more stable than **3**s and **4**s by about 42.6, 22.2 and 29.3 and 34.1 kcal.mol^{-1} for Sn(IV) and Sn(II), respectively. By a closer look at Table 2, it is

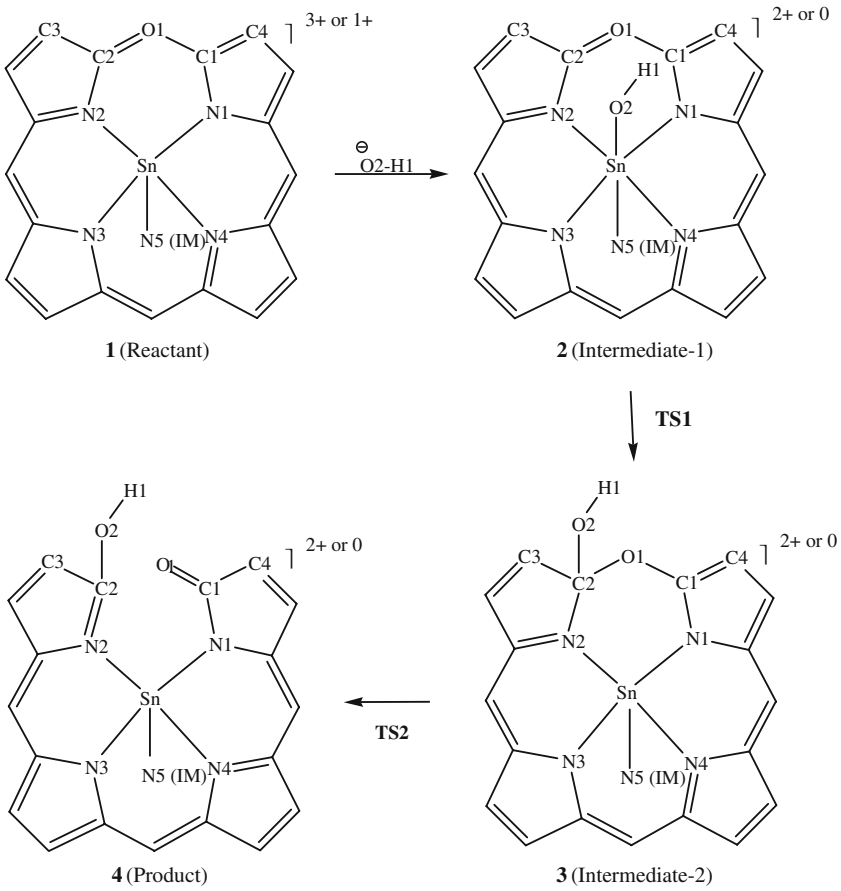

Scheme 3 A perspective view and numbering system of the products of nucleophilic addition of OH^- to five and four coordinate $[Sn^{IV}(OP)(IM)]^{3+}$ or $[Sn^{II}(OP)(IM)]^{+}$ (**1**) as either metal center (**2**), macrocycle (**3**) or as open-chain tetrapyrrol (**4**); Imidazole (IM) is fifth axial ligand in five coordinate complexes

clear that barrier energies for passing over **TS1**s and **TS2**s are 51.9, 73.2 and 8.4, 47.7 kcal.mol^{-1}, respectively.

In accord with previous sections structural data for species **1**s, **2**s, **TS1**s, **3**s, **TS2**s, and **4**s have been summarized in Table 5 which consists of the main geometrical changes in the course of nucleophilic addition of OH^- to **1**s. These selected structural data have been chosen such that comparison with those of six and five coordinated tin verdohemes becomes easier.

Discussion

Hydrolysis of Sn verdohemes: kinetic and thermodynamic point of views

Considering energy values in Table 2 for six coordinate paths, it reveals that open ring helical compounds are more stable than other species. According to traditional transition state theory (TST) [64], rate constants are obtained by following formula:

$$k = \frac{RT}{N_A h} e^{\frac{-\Delta G^{\neq}}{RT}}$$

where, R is the universal gas constant, T is absolute temperature (298K), N_A is Avogadro's constant, h is plank's constant, and $\Delta G^{\neq}$ Gibbs free energy of transition structure. Based on above theory, rate constants for conversion of **3**s to **4**s are of the order of 10^{-13} and 10^{-19} s^{-1} for Sn(IV) and (II), respectively. Considering the latter facts, although the formation of **4**s is affordable from a thermodynamics point of view, they are not favored kinetically and the closed ring hydroxy intermediate-2s are the reaction products in these reactions. It is notable to compare results of six coordinate pathway with results obtained in previous work in OH^- nucleophilic attack to six coordinate bis imidazole Fe(II) verdoheme [43]. The ring opening process in hydroxy verdoheme (**3**) in six coordinate Fe(II) verdoheme was in overall -2.3 kcal.mol^{-1} exothermic with a kinetic barrier of 9.8 kcal.mol^{-1}. Species **3** in six coordinated Fe(II) verdoheme was about 120-130 kcal.mol^{-1} more stable than reactants while in six coordinate Sn(IV) case it increased to 247.8 kcal.mol^{-1}. The more stable intermediate-2 could be related to the presence of Sn in the center of six coordinate tin(IV) verdoheme and highly charged reactants.

Looking at energy values for five coordinate complexes in Table 2 reveals that open ring helical products are a little more stable than other species by amounts of 3.8 and 9.2 kcal.mol^{-1} for Sn(IV) and (II), respectively. Because **2**s are far more stable than **3**s, former species are initially produced in these reactions. By considering TST and data of Table 2, it is clear that rate constants belonging to

conversion of **2**s to **3**s are about 10^{-11} and 10^{-15} s^{-1} respectively. In addition, by referring to rate constants, it is obvious that passing over **TS1**s by rebound mechanism is slower by a factor of about 10^{23} and 10^{16} than passing over **TS2**s, respectively. Regarding these values as well as high barrier energies for passing over **TS1**s, latter conversions, namely production of intermediate-2s are unaffordable processes. Thus, open ring helical compounds are not generated in hydrolysis reactions of five coordinate Sn(IV) and (II) verdohemes. In fact, in the nucleophilic attack of OH^- to five coordinate Sn(IV) and (II) verdohemes, OH^- remains bonded to Sn, and just coordination number of Sn is increased. It is worthwhile to compare results of five coordinate pathway to results obtained in previous work in nucleophilic ring opening in five coordinate Fe(II) verdoheme [43]. There, hydroxide ion attacked the iron center to produce a complex, which was only 1.6 kcal.mol^{-1} more stable than when OH^- directly attacked the macrocycle. The activation barrier for the conversion of iron hydroxy species to the iron biliverdin complex by a rebound mechanism was estimated to be 32.7 kcal.mol^{-1}. In that case, large barrier for rebound mechanism, small barrier of 4.2 kcal.mol^{-1} for ring opening process of the hydroxylated macrocycle, and relatively the same stabilities for complex resulted by addition of nucleophile to the iron and macrocycle were evidenced. Thus it was concluded that five coordinate pathway with direct attack of nucleophile to the 5-oxo positions of macrocycle might be the path for the conversion of verdoheme to biliverdin. The intermediate-1 in five coordinate Fe(II) verdoheme was about 130-150 kcal.mol^{-1} more stable than reactants while in five coordinate Sn(IV) and Sn(II) reactions, it increases to 333.6 and 162.4 kcal.mol^{-1}, respectively. Comparing the energy diagrams of Sn(IV), Sn(II), and Fe(II) pathways show the considerable stability of **2** in Sn relative to Fe which could be related to the presence of highly charged main element of Sn with high oxophilicity and more affinity to increase coordination. Thus, the more stable **2** in five coordinate tin verdoheme could be held responsible for the different energy release in Sn–O bond formation against that of Fe–O. While the more stable **3** may be related to the presence of Sn center with more positive charges in five coordinate tin(IV) verdoheme. Again if we compare results of Sn(II) with Fe(II) verdoheme with the similar oxidation state and coordination, the more stability of **2** in the former case could be accounted as a factor for the prevention of ring opening. Also, it is notable that Sn plays significant coordination role in contrast to its Fe analogue in this path.

By referring to Table 2 for four coordinate pathways and regarding TST, it is disclosed that rate constants for conversion of **2**s to **3**s are of the order of 10^{-25} and 10^{-41} s^{-1} and are slower by a factor of 10^{32} and 10^{17} than formation of products from **3**s for Sn(IV) and (II), respectively. On the other hand, data of Table 2 demonstrates that **2**s are the most stable species in these reactions. Thus, formation of **2**s are more desirable than open ring helical products and **2**s are generated instead of open ring helical products from both thermodynamical and kinetics point of views, when OH^- is added to four coordinate Sn(IV) and (II) verdohemes. In fact, in these nucleophilic additions, similar to the five coordinate counterparts, OH^- is bonded to Sn, and coordination number of Sn is increased. Also, it worth to compare results of four coordinate pathway with results obtained in previous work in nucleophilic attack to four coordinate Zn(II) verdoheme [42]. In nucleophilic addition of hydroxide ion to four coordinate Zn(II) verdoheme, it was determined that **3** is directly converted to helical open-ring complex by passing through **TS2**. There, the intermediate-2 was 0.7 kcal.mol^{-1} more stable than intermediate-1 and 15 kcal.mol^{-1} more unstable than product, respectively. The barrier energy for passing over the **TS2** was 5 kcal.mol^{-1}. The intermediate-1 in four coordinate Zn(II) verdoheme was about 139 kcal.mol^{-1} more stable than reactants while in four coordinate Sn(IV) and Sn(II) complexes, it increases to about 394 and 222 kcal.mol^{-1}, respectively. Comparing the energy diagrams of Sn(IV), Sn(II), and Zn(II) pathways show the considerable stability of **2**s in Sn relative to Zn which could be related to stronger Sn-O bond against Zn-O and presence of highly charged main element of Sn with high oxophilicity and affinity of four coordinate tin for addition of coordination. Thus comparison of Sn(II) to Zn(II) verdoheme with similar oxidation state and coordination number, the higher stability of intermeditae-1 could be accounted responsible as the main factor for ring opening inhibition. It is also notable that similar to five coordinate pathway, Sn plays coordination role in contrast to its Zn analogue.

Comparing the energy stabilities of species and transition states of Sn(II) with the similar Sn(IV) in all pathways shows that Sn(IV) verdohemes have more affinity for increasing coordination state relative to those of Sn(II). Analysis of various pathways verifies that ring opening is less favorable in the latter case, while reduction of oxidation state favors the ring opening prevention. In addition, considering the energy stabilities of species show that four coordinate complexes more avidly increase coordination number than five coordinate analogues.

Hydrolysis of Sn verdohemes: charge analysis

As mentioned in proceeding sections, according to Table 1 charges on Sn in six, five, and four coordinate Sn(IV) and those on Sn(II) are 2.14, 2.01, 1.91, and 2.00, 1.95, 1.73 respectively. While, charges of Fe in six and five coordinate Fe(II) verdohemes have been reported being 1.36 and 1.2

respectively [43] and that for Zn(II) in four coordinate verdoheme equaling 1.22 [42]. Accordingly, more stability of intermediate-1 relative to reactants in nucleophilic attack to five coordinate tin verdohemes could be attributed to more positive charge on Sn, when compared with OH^- addition to Fe(II) verdoheme [43]. Such fact also applies to intermediate-1 in adding OH^- to four coordinate Sn(IV) verdoheme, when compared with Zn(II) verdoheme analogue [42]. Besides the charge differences, some of the aforementioned stability can be accounted for by higher affinity of tin verdohemes for increasing coordination state relative to Zn(II) and Fe(II) verdohemes. Comparing the results of five and four coordinate Sn(II) verdohemes with their Fe(II) and Zn(II) counterparts show that more positive charge on metal center as well as coordination role are two important factors in differentiating the species obtained in hydrolysis pathways. On the other hand, comparison of charges centered on oxo carbon shows no considerable difference. Thus, different charge on Sn center and reactants between six coordinate tin(IV) verdoheme complexes with their tin(II) analogues can demonstrate the considerable stability of intermediate-2 in Sn(IV) complex. The same arguments apply to the higher stability of intermediate-2 in five coordinate tin(IV) verdoheme relative to its tin(II) analogues. Such fact is true in comparison of OH^- attack to four coordinate Sn(IV) with that of four coordinate Sn(II). Moreover, more stability of intermediate-1 in Sn(IV) complexes against their Sn(II) analogues could be related to the more positive charges on Sn(IV) as well as more tendency to increase coordination. Also, comparing stability of intermediate-1 relative to reactants in OH^- addition to five coordinate Sn(IV) with its four coordinate Sn(IV) analogue shows decrease of about 60 $kcal.mol^{-1}$. This trend is similar in comparing the stability of intermediate-1 relative to reactants in five coordinate tin (II) verdoheme and four coordinate tin(II) which again shows decrease of about 60 $kcal.mol^{-1}$ in the hydrolysis pathways. Such observation is indicative of the fact that although Sn(IV) is less positive in four coordinate case, it leads to more stable intermediate. This is suggestive of the significance of liability of Sn in increasing coordination state as key parameter for preventing ring opening. Thus such tendency is decreased from four coordinate Sn to five coordinate Sn as expected. In addition, high barriers for passing over **TS1** in Table 2 could be related to decrease in coordination number of Sn. The coordination issue is discussed further in a forthcoming section.

Hydrolysis of Sn verdohemes: geometrical view

By Taking a look at Table 3 and considering the geometrical parameters related to porphyrin's planarity, it is clear that $[Sn^{IV}(OP)(IM)(OH)]^{2+}$ is an octahedral complex with a planar porphyrin ring. This is in line with the reports on six coordinate tin(IV) as one of the most planar tension free porphyrins [65] which shows the complete accommodation of tin in verdoheme ring. Regarding O3–C2–O1, C2–O3–H1 and N2–C2–O3–H1 angles in intermediate-2, it is determined that OH^- group is not coplanar with its adjacent pyrrole ring. Considerable variations in the porphyrin ring structure of 4 in comparison with that of $[Sn^{IV}(OP)(IM)(OH)]^{2+}$ is seen. Such variations can be summarized as a great increase of C2–O1, decrease in C1–O1 and C1–O–C2, as well as effective variations in N1–Sn–N2, N2–Sn–N4, N2–C2–O1, C3–C2–O1, and C3–C2–O3 angles that are confirmatory of opened helical structure of 4. By regarding C3–C2–O3–H1 value, it becomes obvious that OH^- group is coplanar with its adjacent pyrrole ring in 4. Comparison of differences between values of N1–Sn–N2, N2–Sn–N4 bond angles, as well as N1–N2–N3–N4 dihedral angle in 1 and 4, reveals that the porphyrin ring in 4 has a helical macrocycle structure which is in prefect agreement with experimental result belonging to nucleophilic attack to zinc verdoheme [42]. Table 3 also confirms that structure of the transition states is in accord with expected chemical intuition for conversion of intermediate-2 to product and generation of 3 from 2. To justify this claim, it is found that C2–O1 bond distance has been increased by about 0.37 Å in TS2 relative to 3. Besides, decrease in co-planarity of pyrrole ring adjacent to OH^- group from porphyrin's plane as well as decrease in N2–C2–O3–H1 angle of the transition state relative to that of 3 are indicative of generating an open chain helical structure in 4. In fact, increase of C2–O1 and decrease in C1–O1 show that a biliverdin like species is formed and an open ring product is generated *via* ring opening mechanism. It could be worthwhile mentioning here that as was presented in preceding sections, the aforementioned open ring helical species is not a possible final product. Data of Table 3 reveals that similar trends for structural variations of 1, 3, TS2, and 4, in OH^- addition to six coordinate Sn(II) as those for Sn(IV) verdoheme are observed.

By considering N1–Sn–N3 and N2–Sn–N4 bond angles as well as N1–N2–N3–N4 dihedral in Table 4, it is obvious that Sn atom has moved out of the porphyrin plane in $[Sn^{IV}(OP)(IM)]^{3+}$ and $[Sn^{II}(OP)(IM)]^{+}$. Also, Sn atom has moved to the porphyrin plane after OH^- attaching to latter reactants in the six coordinate **2**s. Variation of Sn–N5 from **3**s to **4**s is observed in reaction of OH^- with **1**s in Scheme 3. Latter fact is due to electron donating ability of imidazole ring. Such ability facilitates C2–O1 bond cleavage. Also, by referring to Tables 4 and 5, it is clear that N1–N2–N3–N4 dihedral is changed considerably from four coordinate Sn verdoheme to five coordinate Sn verdoheme in the presence of imidazole axial ligand. By taking into account geometric parameters belonging to

planarity of macrocycle, it is obvious that intermediate-1 belonging to OH^- addition to five coordinate Sn(II) verdoheme is less planar than that which arises from OH^- attaching to Sn of five coordinate Sn(IV) verdoheme.

Structural data for hydrolysis of four coordinate Sn(IV) and Sn(II) in Table 5 clarifies that $[Sn^{IV}(OP)]^{3+}$ is planar. As can be seen in this table, Sn atom has moved out of the porphyrin plane in **2**s. Delving into Table 5 reveals that structures of **2**, **3**, and **4** of four coordinate Sn(II) are not planar as Sn(IV) verdoheme. Based on these facts, it is expected that intermediates due to addition of OH^- to Sn (II) verdoheme are less stable, when compared with those of Sn(IV) pathway, as illustrated in Table 2. According to Ortiz de Montellano report [66], verdoheme appears flat in crystal structure of verdoheme which complexed with human heme oxygenase protein. Comparison of structures of tin verdohemes studied here show that the structure of full optimized six and four coordinate Sn verdohemes with axially coordinated ligands are more planar than five coordinate. So, they can compete well with iron verdoheme in occupying heme oxygenase protein pocket.

Hydrolysis of Sn verdohemes: oxidation state of Sn

The major difference between structures of tin(IV) and (II) verdoheme complexes can be seen in the coordination sphere of the tin atom. While tin(II) verdoheme complexes are mostly distorted, tin(IV) compounds adopt regular geometries as square planars, square pyramides or octahedrals, depending on the coordination state. The reason for this phenomenon may readily be explained by the different electronic states; while in tin(IV) verdoheme compounds all outer electrons of the tin atom are engaged in bonding, tin (II) verdoheme compounds have one electron pair that does not participate in bonding and displays stereochemical activity. We could consider this electron pair as a further ligand in the coordination sphere of the tin atom in verdoheme complexes. By considering Tables 3, 4, and 5 it can be seen that in general the bond distances in comparable verdoheme compounds are longer for lower oxidation states. The larger Sn(II) bond distances as compared to Sn(IV) can be explained either by a repulsion effect of the lone electron pair at the tin atom, the higher tin's atomic radius, or by weaker bonds compared with tin (IV). Based on Table 1, charge analysis of Sn(IV) and (II) verdohemes shows that except for four coordinate verdohemes, the charge differences is not considerable which may indicate that the main factor in considerable stability of intermediate-1 in Sn(IV) verdohemes relative to Sn(II) verdohemes is not the charge on Sn center. However, it seems that more affinity of Sn(IV) for raising its coordination relative to Sn(II) can be held accountable for that fact. Also, by taking a look at the energy profiles during hydrolysis of various tin verdohemes, it could be concluded that evidently the more oxophilic nature of Sn(IV) makes its Sn–O compounds thermodynamically more stable than those of Sn(II).

Hydrolysis of Sn verdohemes: coordination state of Sn

In the biological and clinical references, it has been shown that the coordination sphere around the tin atom is of paramount importance for the structure of tin(IV) and (II) complexes [67]. Given the fact that the axial ligation of the Sn macrocyclic complexes is often totally ignored in many medically- or biologically-oriented studies in this field [21], it is hoped that our emphasis on these angles may stimulate more detailed appreciation of this fact. The assumption that the ligands on tin porphyrins are chlorides (or even hydroxyls or water in aqueous media) when they are used in biological studies may not always be valid, and this question may be relevant to their efficacy [21].

Sn coordination number is determined largely by Sn ion size, and also to some extent by Sn ion charge. A comparative assessment of the effect of the Lewis acidity of the central tin atom and of ligand basicity on coordination of verdohemes and a summary of Sn–O and Sn–N distances as a function of coordination number and oxidation state can be seen in Tables 3, 4, and 5. The effect of size and charge of the Sn(IV) and (II) and the distances between the tin(II) and (IV) atoms and the ligand when the coordination number is changed as well as inert pair effect (distorted coordination environment for Sn(II) verdoheme compounds) is clearly seen in the mentioned Tables. As expected, these mean distances between the central tin atom and different coordinated atoms (N, O) increase with rising coordination number which is illustrated in Tables 3, 4, and 5 for Sn(IV) pathways. Correlation between tin-ligand distances and coordination numbers is seen in average $Sn–N_{por}$, Sn–N5, and Sn–O2 bond distances in Sn(IV) and Sn(II) verdohemes in different coordination states.

Hydrolysis of Sn verdohemes: analysis of key Kohn-Sham (KS) molecular orbitals

The molecular orbital calculations were carried out for all components involved in hydrolysis pathways of different tin verdohemes. The frontier MOs as shown in Figs. 1 and 2 are selected for the above discussion. Full discussion can be found in the supplementary material for all species involved in various pathways.

KS frontier MOs in six coordinate tin verdohemes

HOMO of OH^- is a p orbital as shown in Fig. 1. Also in this figure, LUMO, LUMO+1 and LUMO+2 of $[Sn^{IV}(OP)$

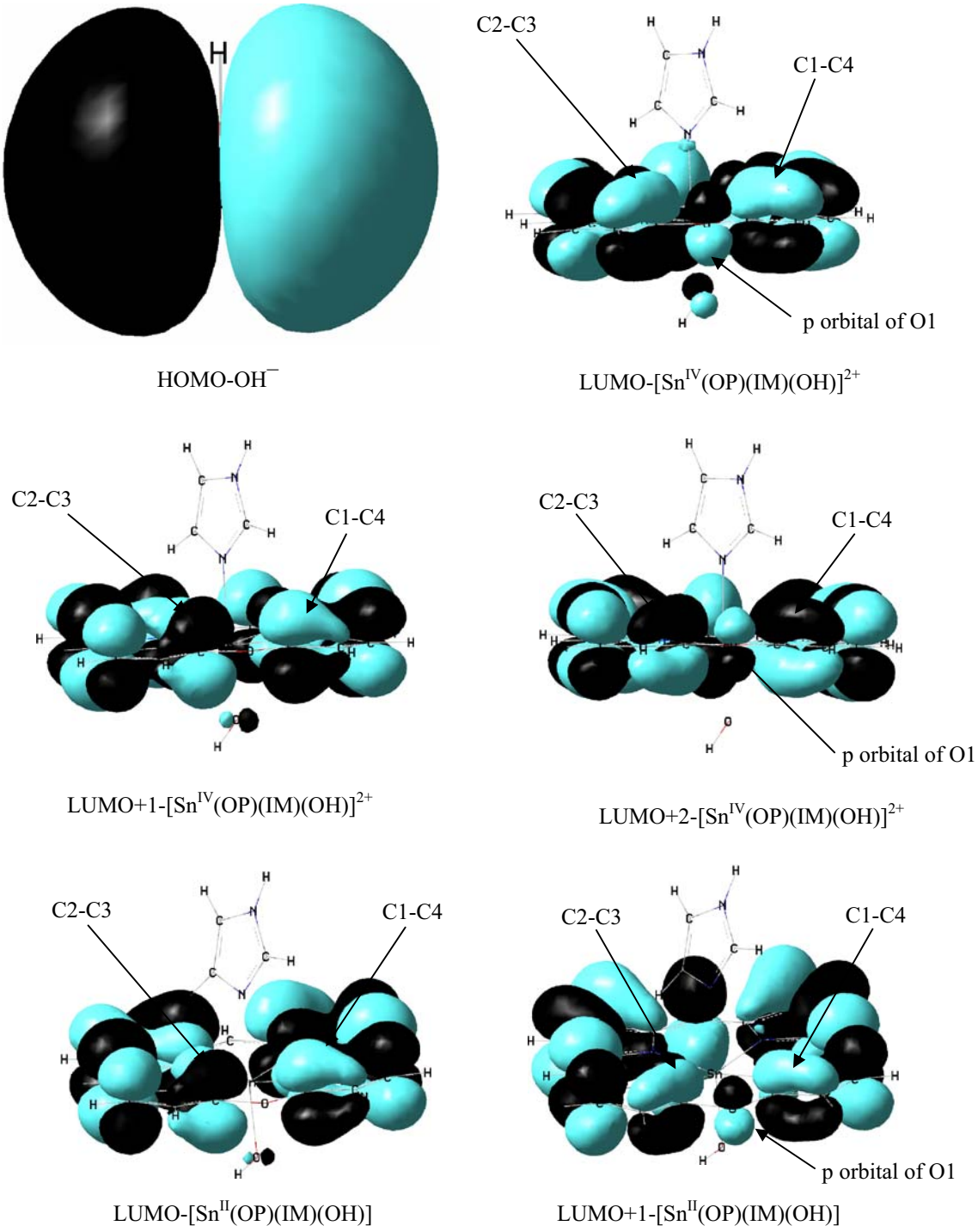

Fig. 1 Selected HOMOs and LUMOs of OH^- nucleophile and six coordinate tin(IV) and (II) verdohemes

$(IM)(OH)]^{2+}$ show a phase combination of p orbitals over C1, C4 as well as C2 and C3. In the LUMO and LUMO+2, such phase combination of p orbitals has an antibonding interaction with p orbital of O1. Thus, HOMO of OH^- can have a bonding interaction with each carbon atoms adjacent to oxygen which can involve effective antibonding interaction with p orbital of O1. Latter fact indicates that p orbital of oxygen atom belonging to $[Sn^{IV}(OP)(IM)(OH)]^{2+}$ has an instability role in leading to probable intermediate. Similar results are obtained by considering MO's belonging to $[Sn^{II}(OP)(IM)(OH)]$ as shown in Fig. 1.

KS frontier MOs in five and four coordinate tin verdohemes

As can be seen in Fig. 2, LUMO of $[Sn^{IV}(OP)]^{3+}$ shows a bonding interaction between p orbital of Sn with two orbitals of two N atoms. In latter MO, a phase combination of p orbitals over C1, C4 and N1 as well as C2, C3 and N2 is observed which has an antibonding interaction with the π-electronic cloud over Sn. Thus, HOMO of OH^- can have a bonding or an antibonding interaction with the π-electronic cloud over Sn or each carbon atoms adjacent to oxygen.

Sn in LUMO of $[Sn^{IV}(OP)(IM)]^{3+}$ has a nonbonding part, and in external LUMO's of this reactant namely, LUMO+4 and LUMO+7 (not shown), a concentrated electronic cloud over tin is observed which has an antibonding interaction with p orbital of N1, N2, N3, and N4 and an electronic cloud belonging to imidazole ring. Thus, HOMO of OH^- interacts with a LUMO of $[Sn^{IV}(OP)(IM)]^{3+}$ involving effective antibonding interaction in the center of verdoheme ring for production of intermediate-1. Therefore, such interaction results in a less stable intermediate-1 relative to reactants, compared with OH^- attack to $[Sn^{IV}(OP)]^{3+}$, as expected. Whereas, in LUMO of $[Sn^{IV}(OP)(IM)]^{3+}$, phase combination between p orbitals of C1 and C4 as well as p orbitals of C2 and C3 is observed which can interact to HOMO of OH^-. This fact results in lowering energy of intermediate-2 relative to intermediate-1, compared with OH^- attack to $[Sn^{IV}(OP)]^{3+}$.

Some MOs belonging to four and five coordinate Sn(II) verdohemes have been illustrated in Fig. 2. A p orbital and concentrated π-electronic cloud has been observed on Sn in LUMO+1 and LUMO+2 (not shown) of $[Sn^{II}(OP)]^+$ respectively. These p orbital and π-electronic clouds have antibonding interaction with π-electronic cloud over N1, N2, N3, and N4. Thus, an intermediate-1 which is produced from interaction of HOMO of OH^- with each LUMOs, will be a less stable intermediate-1 relative to reactants, compared with OH^- attack to $[Sn^{IV}(OP)]^{3+}$. Also, in LUMO of $[Sn^{II}(OP)]^+$ phase combination between p orbitals of C1 and C4 as well as p orbitals of C2 and C3 is observed which can interact to HOMO of OH^-. By taking a look at Fig. 2, reveals that in LUMO of $[Sn^{II}(OP)(IM)]^+$ similar to LUMO of $[Sn^{IV}(OP)(IM)]^{3+}$, phase combination between p orbitals of C1 and C4 as well as p orbitals of C2 and C3 is observed which can interact to HOMO of OH^-. This fact results in lowering energy of intermediate-2 relative to intermediate-1, compared with OH^- attack on $[Sn^{IV}(OP)]^{3+}$. Sn in LUMO of $[Sn^{II}(OP)(IM)]^+$ has a nonbonding part, and in external LUMO's of this reactant namely, LUMO+3 and LUMO+5, concentrated π-electronic cloud and a p orbital on tin is observed respectively, which have an antibonding interaction with p orbital of N1, N2, N3, and N4 and electronic cloud belonging to imidazole ring. Thus, HOMO of OH interacts with a LUMO of $[Sn^{II}(OP)(IM)]^+$ involving effective antibonding interaction in center of porphyrin ring for production of intermediate-1. Thus, as expected such interaction results in a less stable intermediate-1 relative to reactants, compared with OH^- attack to $[Sn^{IV}(OP)]^{3+}$ and $[Sn^{II}(OP)]^+$. Besides, in these LUMOs, phase combination of orbitals of C1 and C4 as well as p orbitals of C2 and C3 is observed which can interact to HOMO of OH^-.

Preventing verdoheme ring opening: role of tin metal

The leading inhibitors of heme oxygenase are the tin porphyrins and they have been successfully established as drug for competitive inhibition of heme oxygenase [23–31]. In addition, possible implications for inhibition of ring opening by high valent tin porphyrins therapeutics have not been described completely. Our previous reports showed that the Zn(II) and Fe(II) verdohemes hydrolysis lead to ring opening and biliverdin complexes formation, while the presented results in this paper show that tin verdohemes ring opening is inhibited. There are several reasons, which make tin porphyrins such interesting therapeutics, the most important being the well known high oxophilicity of the hard tin atom. This is in contrast to the commonly studied metalloporphyrin complexes of the middle and late transition metals, which generally display a higher affinity for binding to ligands with nitrogen donor atoms. It is also known that hypercoordination of a main-group element such as Sn strongly influences its reactivity and may be used to promote coordination behavior. The use of the axial positions of these metalloporphyrins provides ample opportunities to reach this goal. In addition, tin porphyrins are extremely stable and do not release the metal even under harsh conditions [68]. In many ways Sn verdoheme complexes are the ideal candidates in this regard, because of their different coordination state. It is generally true that the higher the charge density, the greater is the ability of the Lewis acid such as Sn to attract the negative charge. In this work, we focused on the high valent oxophilic chemistry of tin porphyrins as a means to attach additional group that allow for further structural extension in a facile manner. One such way is by tin coordination chemistry which in order to be compatible with the tin verdohemes, should rely on metal-ligand interaction. We described interactions of Sn verdohemes that bind oxygen-based ligands and for which the Sn–O bond is in slow exchange on the rebound mechanism and hence preventing their ring opening. As far as the coordination around the peripheral tin atoms is concerned, the oxophilicity of the tin center accounts for these unprecedented features. The exclusive oxophilicity of the tin atom and its high affinity for increasing coordination state promote it as a hard center preferring interactions with

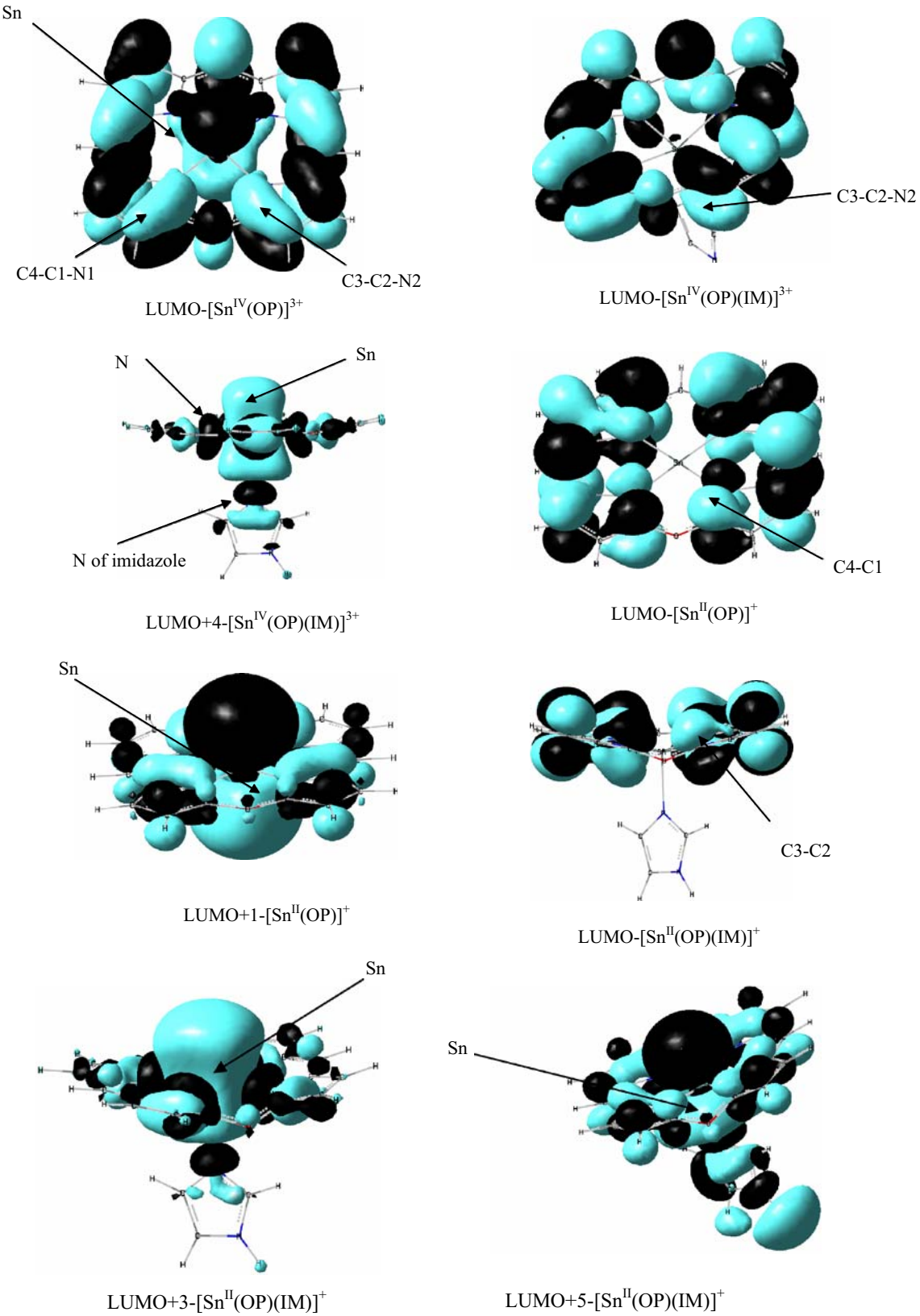

Fig. 2 Selected LUMOs of five and four coordinate tin(IV) and (II) verdohemes

hard molecules such as oxygen or O-bonded ligands such as OH^- which could be the basis for the therapeutic action of Sn porphyrins in its competitive inhibition of heme oxygenase.

Summary and conclusions

In an effort to investigate possible implications for the inhibition of ring opening mechanism in tin verdoheme degradation, three possibly six, five, and four coordinate verdoheme complexes of tin(IV) and (II) have been studied by hydrolysis pathway using B3LYP method. The results of calculations suggest that in excellent agreement with experimental reports, hydrolysis of various possible coordinated tin(IV) and (II) verdohemes does not conduce to the opening of the macrocycle and the hydrolysis reaction of the tin porphyrins is stopped at verdoheme in contrast to the Fe(II) and Zn(II) verdohemes analogues. It is determined that in saturated six coordinate tin(IV) and (II) verdoheme complexes, tin has no coordination role and direct addition of hydroxide ion to the positive oxo-carbon centers and formation of closed ring hydroxy compounds is proposed for blocking the verdoheme center and preventing ring opening. In this path although the ring opening is thermodynamically afforded, it is disfavored kinetically. Also, four coordinate tin verdohemes attract nucleophile more avidly than five coordinate complexes. In hydrolysis reaction of four coordinate Sn(IV) and (II) verdohemes, ring opening does not occurr from both thermodynamics and kinetics point of views. Also, same reasoning applies to the reaction of OH^- with five coordinate Sn(IV) and (II) verdohemes. Contrary to zinc and iron verdohemes, in five and four coordinate verdoheme complexes of tin(IV) and tin(II) the binding of hydroxide to tin metal due to the highly charged oxophilic nature of the Sn center, and high affinity to increase coordination number are the proposed factors responsible for inhibiting the verdoheme ring opening. Comparing results of Sn(II) pathways with those of Sn(IV) show that the ring opening is less favorable in former paths, and reduction of oxidation states stimulates the ring opening inhibition.

In addition, among the metal complexes, the six and four coordinated complexes maintain their planar structures by utilizing imidazole and a hydroxyl as the axial ligands and possibly could compete in occupying HO cavity. Hence, despite the simplicity of the model, the agreement with clinical and medical trials is highly satisfying and the concept of the importance of metal substitution on the observed inhibition of the verdoheme ring opening is fully confirmed. Accordingly, theoretical evidences which have been presented here for the inhibiting reaction cleared some mechanistic aspects of HO inhibition by tin porphyrin drug candidates based on the exclusive oxophilicity of tin porphyrins during hydrolysis pathway of tin verdohemes. The remarkable results of interaction between tin verdohemes and hydroxide nucleophile could evidence a great interest in tin porphyrin analogues as interventional agents for neonatal hyperbilirubinemia.

Acknowledgments We are grateful to Prof. S.W. Ng for providing us the G98W software and hardware (machine time) facilities. The financial support of Research Council of Shahid Beheshti University is gratefully acknowledged. Mehdi D. Davari would like to thank Professor Masato Noguchi, Department of Medical Biochemistry, Kurume University School of Medicine, for his helpful discussions.

References

1. Ortiz de Montellano PR (1998) Acc Chem Res 31:543-549
2. Yoshida T, Migita CT (2000) J Inorg Biochem 82:33–41
3. Colas C, Ortiz de Montellano PR (2003) Chem Rev 103:2305-2332
4. Kikuchi G, Yoshida T, Noguchi M (2005) Biochem Biophys Res Commun 338:558–567
5. Unno M, Matsui T, Ikeda-Saito M (2007) Nat Prod Rep 24:553–570
6. Liu Y, Ortiz de Montellano PR (2000) J Biol Chem 275:5297–5307
7. Lagarias JC (1982) Biochim Biophys Acta 717:12–19
8. Balch AL, Latos-Grazynski L, Noll B C, Olmstead MM, Szterenberg L, Safari N (1993) J Am Chem Soc 115:1422–1429
9. Balch AL, Koerner R, Latos-Grazynski L, Lewis JE, St Claire TN, Zovinka EP (1997) Inorg Chem 36:3892–3897
10. Avila L, Huang Hung-Wei, Damaso CO, Lu S, Moenne-Loccoz P, Rivera M (2003) J Am Chem Soc 125:4103-4110
11. Rivera M, Zeng Y (2005) J Inorg Biochem 99:337–354
12. Matsui T, Nakajima A, Fujii H, Matera KM, Migita KT, Yoshida T, Ikeda-Saito M (2005) J Biol Chem 280:36833–36840
13. Matsui T, Omori K, Jin H, Ikeda-Saito M (2008) J Am Chem Soc 130:4220–4221
14. Balch AL, Koerner R, Olmstead MM, Safari N, St Claire TN (1995) J Chem Soc Chem Commun 6:643–644
15. Lad L, Friedman J, Li H, Bhaskar B, Ortiz de Montellano PR, Polous TL (2004) Biochemistry 43:3793-3801
16. Koerner R, Latos-Grazynski L, Balch AL (1998) J Am Chem Soc 120:9246–9255
17. Johnson JA, Olmstead MM, Stolzenberg AM, Balch AL (2001) Inorg Chem 40:5585–5595
18. Latos-Grazynski L, Johnson J, Attar S, Olmstead MM, Balch AL (1998) Inorg Chem 37:4493–4499
19. Johnson JA, Olmstead MM, Balch AL (1999) Inorg Chem 38:5379–5383
20. Drummond GS, Kappas A (1981) Proc Natl Acad Sci USA 78:6466–6470
21. Arnold DP, Blok J (2004) Coordin Chem Rev 248:299–319
22. Louie AY, Meade TJ (1999) Chem Rev 99:2711–2734
23. Drummond GS, Kappas A (1982) Science 217:1250–1252
24. Kappas A, Drummond GS (1986) J Clin Invest 77:335–339
25. Sardana MK, Kappas A (1987) Proc Natl Acad Sci USA 84:2464–2468
26. Rubaltelli FF, Dario C, Zancan L (1995) Pediatrics 95:942–944
27. Martinez JC, Garcia HO, Otheguy LE, Drummond GS, Kappas A (1999) Pediatrics 103:1–5
28. Dennery PA, Seidman DS, Stevenson DK (2001) N Engl J Med 344:581–589

29. Kappas A, Drummond GS, Valaes T (2001) Pediatrics 108:25–30
30. Wong RJ, Bhutani VK, Vreman HJ, Stevenson DK (2007) Neoreview 8:77–84
31. Breslow E, Chandra R, Kappas A (1986) J Biol Chem 261:3135–3141
32. Morgan WT, Alam J, Deaciue V, Muster P, Tatum DM, Smith A (1988) J Biol Chem 263:8226–8231
33. Deeb RS, Peyton DH (1991) J Biol Chem 266:3728–3733
34. Davydov RM, Yoshida T, Ikeda-Saito M (1999) J Am Chem Soc 121:10656–10657
35. Matsui T, Kim SH, Jin H, Hoffman BM, Ikeda-Saito M (2006) J Am Chem Soc 128:1090–1091
36. Kamachi T, Shestakov AF, Yoshizawa K (2004) J Am Chem Soc 126:3672–3673
37. Kamachi T, Yoshizawa K (2005) J Am Chem Soc 127:10686–10692
38. Kumar D, Hirao H Jr, LQ SS (2005) J Am Chem Soc 127:8204–8213
39. Chen H, Moreau Y, Derat E, Shaik S (2008) J Am Chem Soc 130:1953–1965
40. Meunier B, de Visser SP, Shaik S (2004) Chem Rev 104:3947–3980
41. Poulos TL (1988) Pharm Res 5:67–75
42. Bahrami H, Zahedi M, Safari N (2006) J Inorg Biochem 100:1449–1461
43. Gheidi M, Safari N, Bahrami H, Zahedi M (2007) J Inorg Biochem 101:385-395
44. Land EJ, McDonagh AF, McGravey DJ, Truscott TG (1988) Proc Natl Acad Sci USA 85:5249–5253
45. Ghosh A (2000) J Porphyr Phthalocya 4:380–381
46. Ghosh A (2006) J Biol Inorg Chem 11:671–673
47. Neese F (2006) J Biol Inorg Chem 11:702–711
48. Zahedi M, Bahrami H, Shabazian S, Safari N (2003) THEOCHEM 633:21–23
49. Jamaat P R, Safari N, Ghiasi M, Naghavi S Sh, Zahedi M (2008) J Biol Inorg Chem 13:121-132
50. Sy Dy E, Kasai H (2006) Chem Phys Lett 422:539-542
51. Iwamoto H, Horib K, Fukazawa Y (2006) Tetrahedron 62:2789–2798
52. Becke AD (1993) J Chem Phys 98:5648-5652
53. Becke AD (1988) Phys Rev A 38:3098-3100
54. Lee C, Yang W, Parr RG (1988) Phys Rev B 37:785–789
55. Binkley JS, Pople JA, Hehre WJ (1980) J Am Chem Soc 102:939–947
56. Ditchfield R, Hehre WJ, Pople JA (1971) J Chem Phys 54:724–728
57. Peterson GA, Al-Laham MA (1991) J Chem Phys 94:6081–6090
58. Frisch MJ, Trucks GW, Schlegel HB, Scuseria GE, Robb MA, Cheeseman JR, Zakrzewski VG, Montgomery JA, Stratmann RE, Burant JC, Dapprich S, Millam JM, Daniels AD, Kudin KN, Strain MC, Farkas O, Tomasi J, Barone V, Cossi M, Cammi R, Mennucci B, Pomelli C, Adamo C, Clifford S, Ochterski J, Petersson GA, Ayala PY, Cui Q, Morokuma K, Malick DK, Rabuck AD, Raghavachari K, Foresman JB, Cioslowski J, Ortiz JV, Stefanov BB, Liu G, Liashenko A, Piskorz P, Komaromi I, Gomperts R, Martin RL, Fox DJ, Keith T, Al-Laham MA, Peng CY, Nanayakkara A, Gonzalez C, Challacombe M, Gill PMW, Johnson B, Chen W, Wong MW, Andres JL, Gonzalez C, Head-Gordon M, Replogle ES, Pople JA (1998) Gaussian 98. Gaussian Inc, Pittsburgh, PA
59. Boys SF, Bernardi F (1970) Mol Phys 19:553–566
60. Hay PJ, Wadt WR (1985) J Chem Phys 82:299–310
61. Host JR, Takahashi S, Wang J, Rousseau DL, Ishikawa K, Yoshida T, Ikeda-Saitot M (1994) J Biol Chem 269:1010–1014
62. Lad L, Friedman J, Li H, Bhaskar B, Ortiz de Montellano PR, Poulos TL (2004) Biochemistry 98:1686-1695
63. Szterenberg L, Latos-Grazynski L, Wojaczynski J (2003) Chem Phys Chem 4:691–698
64. Eyring H, Polanyi M (1931) Z Phys Chem Abt B 12:279–311
65. Hoard JL (1975) In: Smith KM (ed) Porphyrins and Metalloporphyrins. Elsevier, Amsterdam, p 317
66. Lad L, Ortiz de Montellano PR, Poulos TL (2004) J Inorg Biochem 98:1686–1695
67. Veith M, Recktenwald O (1982) Topics in Current Chemistry, Organotin Compounds. Springer, Berlin, 104: pp 1–55
68. Keinana E, Sinhaa SC, Sinha-Bagchia A, Benorya E, Ghozib MC, Eshharb Z, Greenc BS (1990) Pure Appl Chem 62:2013–2019